Eur. Phys. J. B **51**, 79–85 (2006)
DOI: 10.1140/epjb/e2006-00200-4

THE EUROPEAN PHYSICAL JOURNAL B

Activation energy in $La_{0.7}Ca_{0.3}MnO_3/YBa_2Cu_3O_{7-\delta}/La_{0.7}Ca_{0.3}MnO_3$ superconducting trilayers

M. Salvato[1,a], F. Bobba[2], G. Calabrese[2], C. Cirillo[2], A.M. Cucolo[2], A. De Santis[2], A. Vecchione[2], and C. Attanasio[2]

[1] Dipartimento di Fisica, Università degli Studi di Roma Tor Vergata, 00133, Roma, Italy and INFM-Laboratorio Regionale SuperMat, 84081, Baronissi, Salerno, Italy
[2] Dipartimento di Fisica "E.R. Caianiello", Università degli Studi di Salerno and INFM-Laboratorio Regionale SuperMat, I-84081, Baronissi, Salerno, Italy

Received 1st February 2006 / Received in final form 16 March 2006
Published online 31 May 2006 –

Abstract. Resistivity vs. temperature measurements on $La_{0.7}Ca_{0.3}MnO_3/YBa_2Cu_3O_{7-\delta}/La_{0.7}Ca_{0.3}MnO_3$ (LCMO/YBCO/LCMO) trilayers with different YBCO thickness, were performed in external magnetic field H up to 8 T. By evaluating the activation energy U from the slope of the resistivity Arrhenius plot, a strong depression of U has been observed when decreasing the YBCO layer thickness and the absolute U values appear to be reduced with respect to the values reported in literature in the case of YBCO thin films and YBCO/insulating multilayers. Moreover, a logarithmic U vs. H dependence is shown both in the case of thick and thin YBCO layers indicating the formation of a two dimensional vortex lattice. The experimental data are discussed considering the strong influence of the ferromagnetic LCMO on the superconducting YBCO properties which reduces the effective YBCO thickness more than predicted by the conventional theories.

PACS. 74.25.Qt Vortex lattices, flux pinning, flux creep – 75.47.Lx Manganites – 74.78.Fk Multilayers, superlattices, heterostructures

1 Introduction

The coexistence between superconductivity and magnetism has been an interesting issue of study since many years [1]. Artificial structures formed by superconducting (S) layers alternately stacked with ferromagnetic (F) layers have been routinely obtained by different deposition methods and their properties have been widely studied especially in the case of metallic S and F materials. Proximity effect theory, modified by the contribution of the interface transparency and the presence of an exchange integral in the F layers, has been applied to the S/F systems giving a qualitative and, in many cases, a quantitative explanation of the different observed phenomena [2]. As an example, the non-monotonic decrease of the critical temperature T_c as a function of the F layers thickness and the existence of a finite critical thickness of the S layers, defined as the minimum thickness which allows the superconductivity to be sustained, have been predicted [3,4] and experimentally confirmed [5]. Recently, the interest in S/F structures has been extended to systems in which the two constituents are an high-T_c superconductor (HTS) and a fully spin-polarized ferromagnetic manganite [6–8]. On these structures a lot of investigations have been performed: scanning tunneling spectroscopy [9], tunneling magnetoresistance [10], analysis of the far-infrared properties by ellipsometry [11]. Moreover, possible applications such as F/S/F spin valves [12] and π-junctions [13] as well as spin polarized quasi particles injection devices have been considered [14].

For these systems, superconducting critical temperature measurements in the absence of an external magnetic field have given the experimental evidence of the strong influence of the F layers on the superconducting properties of the S layers which is alternatively interpreted as long range proximity effect, injection of quasiparticles from F to S or both [6,7,15]. Whatever the cause of the observed T_c depression, the influence of the F layer is shown to be effective deep inside the S layer up to a distance l_S which is much longer than the Ginzburg-Landau superconducting coherence length ξ_S whose value is about 3 Å for $YBa_2Cu_3O_{7-\delta}$ (YBCO). This gives rise to the existence of a superconducting critical thickness of about 30 Å which is, on one hand, shorter than the value measured in metallic S/F multilayers [15], but much longer than $2\xi_S$ in contrast with the commonly accepted S/F theories.

Besides all these interesting phenomena, the use of HTS as S layers opens new scenarios on the possibility to study the effect of ferromagnetism on the dissipative

[a] e-mail: matteo.salvato@roma2.infn.it

phenomena which are present in superconductors. In particular the influence of the vortex motion on the resistivity transition can be easily evidenced in these materials because of the large separation between the upper critical field and the Irreversibility Line (IL) in the $H-T$ phase diagram. In this range of field (H) and temperature (T), the vortex dynamics can be influenced by the presence of an F layer giving rise to new intriguing mechanisms related to the dimensionality of the vortex lattice.

The dimensionality of the vortex lattice has been widely studied in both low and high temperature superconductors as well as in artificial heterostructures based on these materials [16–19]. One of the methods used to distinguish between a 2-dimensional (2D) or a 3-dimensional (3D) formation of the vortex lattice is the study of the dependence of the activation energy U from the external magnetic field. Strictly speaking, a $U \sim H^{-\alpha}$ dependence is commonly observed with the exponent $\alpha = 0.5$ or $\alpha = 1$ for the 2D and 3D cases respectively [20]. However, some other relations between U and H have been reported as well as the appearance of different regimes with the variation of H [21–24]. Among them, the presence of 2D pancake vortices gives rise to a $U \sim -\log H$ dependence which is usually ascribed to the formation of pair dislocations in the vortex lattice and gives evidence of the formation of a 2D regime [25].

Concerning the HTS based heterostructures, most of experimental work present in the literature deals with $YBa_2Cu_3O_{7-\delta}/PrBa_2Cu_3O_7$ (YBCO/PrBCO) superlattices where the effects of the presence of the PrBCO insulating layers has been studied on the vortex dynamics by changing both the PrBCO and YBCO thickness [26–29]. Beside the reduction of the critical temperature, a depression in the irreversibility line (IL) and in the activation energy U has been observed with respect to YBCO bulk samples due to the reduction of the YBCO layer thickness [27–29]. These effects have been interpreted as an enhancement of the thermal and quantum fluctuations and as a reduction of the dimensionality of the vortex lattice both due to the decoupling between the superconducting layers operated by the insulating layers. However, the effect is comparable to that observed in the case of YBCO thin films and it is mainly attributed to the reduction of the YBCO layers thickness rather than the influence of the insulating PrBCO layers [27]. Moreover, in the case of YBCO thin films and YBCO/PrBCO multilayers, a linear dependence of U from the YBCO layer thickness [27,28] has been observed for thickness smaller than 450 Å which corresponds to the vortex correlation length L_c in the direction of the applied field. As a result, the vortex lattice is considered to be in a 2D or 3D regime when the layer thickness is lower or higher than L_c respectively [19]. In contrast to this little has been done regarding the investigation of the activation energy U and the vortex lattice behavior in F/YBCO/F layered structures to explicitly evaluate the role played by the ferromagnetic layer on the superconducting properties of the entire system.

In the following, we study the magnetic field dependence of the activation energy for two $La_{0.7}Ca_{0.3}MnO_3/YBa_2Cu_3O_{7-\delta}/La_{0.7}Ca_{0.3}MnO_3$ (LCMO/YBCO/LCMO) samples with YBCO layer thickness (d_{YBCO}) of 160 Å and 660 Å which correspond to the cases $d_{YBCO} < L_c$ and $d_{YBCO} > L_c$. Comparing our results with those obtained for YBCO/PrBCO multilayers [26–28], we maintain that the presence of the F layers, apart from reducing the critical temperature values, causes also a decrease of the value of the activation energy and of the dimensionality of the vortex lattice even in the sample with the YBCO thicker layer where a 3D regime is expected.

2 Samples fabrication and experimental procedure

The LCMO/YBCO/LCMO trilayers were fabricated on $SrTiO_3$ (001) (STO) single-crystal substrates by multitarget high pressure dc sputtering. Two targets with nominal composition of $La_{0.7}Ca_{0.3}MnO_3$ and $YBa_2Cu_3O_{7-\delta}$ were used for depositions. During the growth, the temperature of the substrate was set at 800 °C and the oxygen pressure was kept at 3.0 mbar for both the LCMO and YBCO layers. The thickness of the layers was controlled by the sputtering time of the respective materials. The calibrated growth rates were about 3 Å/min for LCMO and 17 Å/min for YBCO. After the deposition, the samples were in-situ annealed for one hour at 560 °C in an oxygen pressure of 1 bar. The deposited films were then cooled to room temperature with a rate of 10 °C/min. Trilayers with the same LCMO thickness and different YBCO thickness have been routinely obtained and grown in the same conditions.

The structural properties of the samples have been studied by a high resolution X-ray diffractometer equipped with a graded parabolic mirror and a Ge(220) four crystals asymmetric monochromator on the primary arm to have a monochromatic $Cu_{K\alpha 1}$ beam with $\lambda = 1.54056$ Å. In order to estimate the interface roughness, reflectivity measurements have been performed on test samples with the same apparatus using a 20-sheets parallel beam collimator with a 0.1 mm slit placed in front of the detector, giving a diffracted beam divergence less than 0.1°. As an example, in Figure 1 is shown the reflectivity spectrum of a trilayer LCMO/YBCO/LCMO with $d_{LCMO} = 245$ Å and $d_{YBCO} = 395$ Å. The presence of the interference fringes confirm that the layering structure has been obtained. Also shown in Figure 1 is a simulated spectrum, shifted below the experimental one, obtained by using a simulation program [30,31] in which the thickness and the density of the expected layers, obtained by the sputtering time and by literature data respectively, were introduced. The fitting procedure allowed to estimate a roughness at the interfaces of about 6 Å and confirmed that no different phases or oxide compounds were formed at the interface between the different layers and on the substrate surface.

The resistivity vs. temperature measurements have been performed in a standard liquid Helium cryostat equipped with a superconducting magnet thermally decoupled from the holder so as to change both the sample

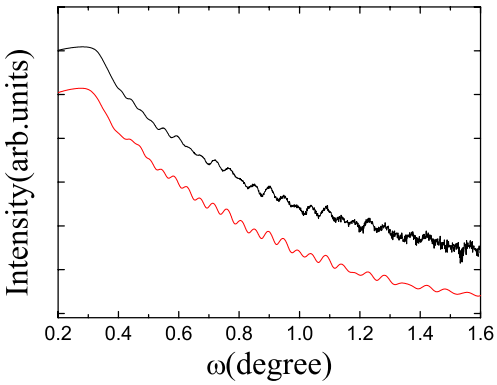

Fig. 1. Experimental X-ray reflectivity measurement (upper curve) for a test LCMO/YBCO/LCMO trilayer with $d_{LCMO} =$ 245 Å and $d_{YBCO} = 395$ Å. Simulated spectrum (lower curve) obtained assuming no oxide at the interfaces.

temperature (from 300 K to 4.2 K) and, independently, the magnetic field up to 9 T. The direction of the magnetic field was fixed perpendicular to the substrate surface and to the direction of the circulating current.

The resistivity data in external magnetic field presented in this paper refer to two LCMO/YBCO/LCMO trilayers named LYL1 and LYL2. Both have LCMO thickness greater than 150 Å while the YBCO layers are 160 Å and 660 Å thick, respectively.

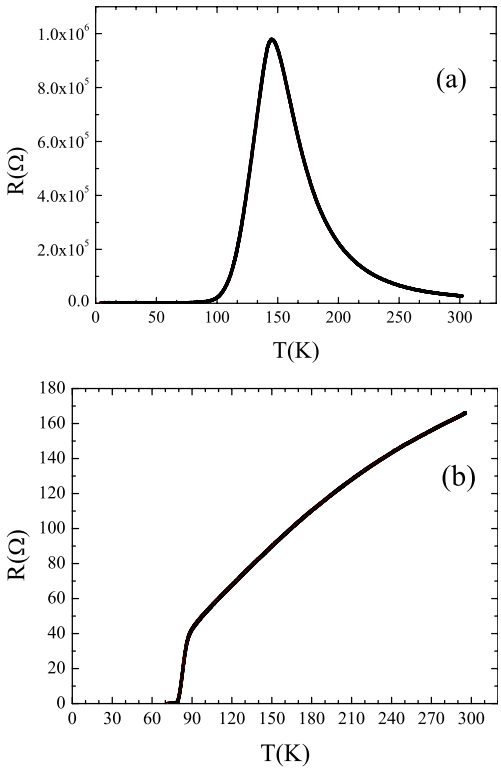

Fig. 2. Resistance vs. temperature for (a) 80 Å thick LCMO film showing $T_{MI} = 145$ K and $T_M = 125$ K and (b) 100 Å thick YBCO film with $T_c = 78$ K deposited separately on STO substrates.

3 Experimental results

Figure 2a shows the resistance vs. temperature of a 80 Å LCMO film deposited on a STO substrate. A semiconducting-metallic cross-over temperature $T_{MI} =$ 145 K is present. As usually observed in these materials, the Curie temperature (T_M) is slightly lower than T_{MI} and corresponds to the minimum in the first derivative of the R vs. T line. In the case of Figure 2a, this value is 125 K. Due to strain effects induced by the lattice mismatch with the substrate [32], both T_{MI} and T_M are lower than the bulk values which are above 250 K for optimally doped LCMO. The resistance vs. temperature behavior of a 100 Å thick YBCO film deposited on STO substrate is reported in Figure 2b showing a superconducting transition at $T_c(R = 0) = 78$ K and a transition width $\Delta T \cong 5$ K. The reduced T_c and the increased transition width with respect to the bulk value ($T_c = 92$ K and $\Delta T \cong 1$ K respectively) are mainly due to the reduced thickness of the samples.

In order to study the crystal structure of the different layers and the epitaxial relation between them and with the substrate, in-plane and out-of-plane X-ray diffraction measurements have been performed. In Figure 3a the ϑ–2ϑ spectrum of the LYL2 sample is reported, showing that the substrate and the layers are all (00l) oriented. The inset shows an enlarged part of the spectrum with the (002) peaks of STO and LCMO and the (006) peak of YBCO. From the position of the diffraction peaks the c-axis lengths for LCMO and YBCO, $c_{LCMO} = 3.823$ Å and $c_{YBCO} = 11.697$ Å have been obtained. The epitaxial growth is confirmed by the in-plane $h - l$ reciprocal space map, reported in Figure 3b for the same sample, which shows that the in-plane axes of the substrate and of the LCMO and YBCO layers are all in the same direction. Measuring the in plane lattice constants we obtained $a_{LCMO} = 3.90$ Å (the same as STO inside the experimental uncertainty) and $a_{YBCO} = 3.83$ Å which indicates that LCMO grows tensile strained on STO whereas YBCO is structurally more relaxed as expected. The possible presence of a strained LCMO layer on the YBCO structure, as found by other authors [33], is not clearly evidenced in our maps. We will discuss this effect elsewhere but we argue that the X-ray diffraction measurements confirm that all the layers are epitaxial and that LCMO layers grow with the a-axis longer than the bulk value ($a_{bulk} = 3.859$ Å).

Figures 4a and 4b show the resistance vs. temperature in external magnetic field up to 8 T for the samples LYL1 and LYL2 respectively. The reduction of the thickness in the YBCO layers involves a decrease in the critical temperature of the trilayers in zero field from $T_c = 48.5$ K to $T_c = 19.5$ K. Moreover the width of the resistive transitions in zero field is wider for the sample with the thinnest YBCO layer and, for both the samples, it is wider than that shown in Figure 2b measured for a single thin YBCO film. The resistive transitions broaden in the low temperature region with the applied field as expected for HTS. Taking the values of the fields and temperature at 90%

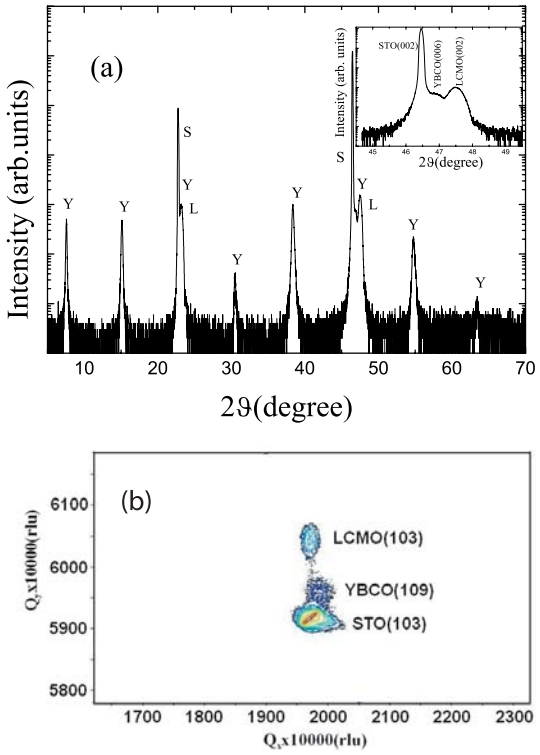

Fig. 3. (a) ϑ-2ϑ X-ray diffraction spectrum for the LYL2 sample where Y, L, S indicate YBCO, LCMO and substrate Bragg diffraction peaks, respectively. The inset shows the part of the spectrum containing the (002) substrate and LCMO peaks and the (006) YBCO peak. (b) $h-l$ reciprocal space map for the same sample with Q_x and Q_y the in plane and out of plane reciprocal space vectors respectively.

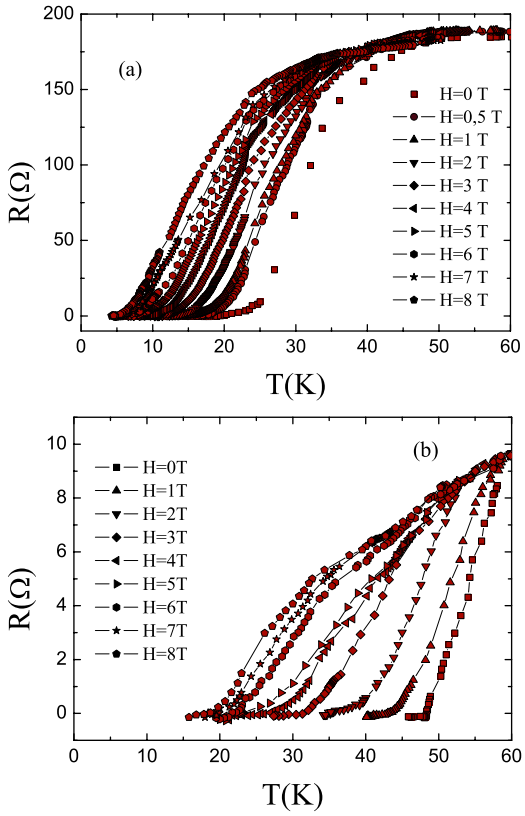

Fig. 4. Resistance vs. temperature data for the samples LYL1 (a) and LYL2 (b) in perpendicular external magnetic field. The values of the field are reported in the figures.

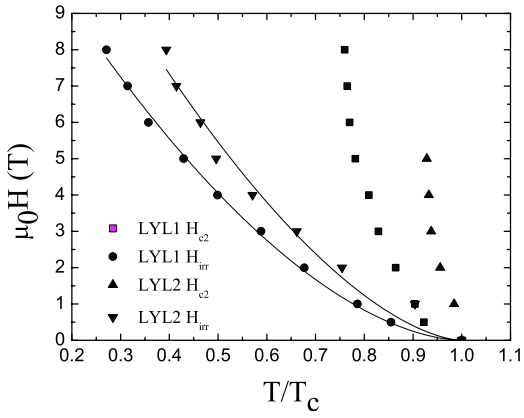

Fig. 5. $H-T$ phase diagram showing the upper critical fields and the IL vs. temperature dependence obtained from the data of Figure 4 for the two samples. The lines are fit to the data assuming a power law dependence for the IL with exponents $n = 1.7$ and $n = 1.6$ for LYL1 and LYL2 respectively.

of the normal state resistance R_N, the upper critical field H_{c2} vs. temperature dependence has been obtained and shown in Figure 5. An upward curvature, probably due to the presence of thermal fluctuations [34], is present for both the samples which is different from that observed in the case of HTS where a linear Ginzburg-Landau (GL) dependence is shown at least near T_c. Also shown in Figure 5 is the IL (H_{irr} vs. T) obtained taking the field and temperature values when $R = 0.1R_N$. Although this method is not rigorous for the determination of the IL, it gives an indication of the lower boundary of the dissipation region in the $H-T$ phase diagram. Due to the rather noisy resistance curves, the ILs are well approximated by a power law temperature dependence $H_{irr} \sim (1 - T/Tc)^n$ with $n = 1.7 \pm 0.1$ and 1.6 ± 0.1 for LYL1 and LYL2 samples respectively. Other approximations following the different models existing in literature for H_{irr} vs. T [35] do not give a unique result in the whole range of the data. The value of $n \cong 3/2$ found for the exponents in the case of our samples suggests that the dissipation region (above the IL) is governed by thermally activated flux flow (TAFF) [18,26,29].

The same data of Figure 4 are reported in Arrhenius fashion in Figures 6a and in 6b. We argue that below 1% of the normal state resistance R_N, the resistivity appears thermally activated with $R = R_N \exp(-U^*/k_BT)$ where U^* is an effective activation energy which depends on the magnetic field and temperature and k_B is the Boltzmann constant. The U^* values are obtained from the Arrhenius plot data calculating the slope of the curves in the low temperature region. These values are, at least in principle, temperature dependent due to the change in the slope of the Arrhenius data with T. The real activation energy

U of the samples is then reduced with respect to U^* by a temperature dependent factor [20]. Therefore, if one wants to determine the U value starting from the U^* measurements, the U vs. T dependence determination is necessary. Several models have been proposed [35–37] which are based on the GL hypothesis of a linear dependence of H_{c2} vs. temperature which is not our case as shown in Figure 5. For this reason, our discussion will be focused on the U^* data instead of U values, taking into account that U^* is higher than U for a given magnetic field. In Figure 7 the U^* values are reported as a function of the magnetic field in a semilogarithmic plot for both the investigated samples. The experimental data are well approximated in the entire range of measurements by a linear regression giving the dependence $U^* = -k \log H + \beta$, with k and β constant, for each sample. The typical power law dependence $U^* \sim H^{-\alpha}$ does not fit our data in the whole magnetic fields range but gives at least two regimes with unphysical values of the exponent α. Moreover, the values of U^* are smaller than 200 meV for the sample with the thicker YBCO layer and they are strongly reduced for the thinner YBCO layer. In addition, these values are much smaller than those observed in YBCO thin films [37] and in YBCO/PrBCO multilayers [27,28] with comparable YBCO thickness layers.

4 Discussion

The effects of the coupling between magnetic and superconducting layers can be appropriately studied if the single LCMO and YBCO layers present magnetic and superconducting properties at least in the range of the investigated temperatures which extend below 50 K as shown in Figure 4. This is the case of our samples as indicated in the data in Figure 2 which refer to 80 Å LCMO and 100 Å YBCO thin films separately deposited on STO substrates. The depression in T_{MI} and T_M in LCMO thin films with respect to the bulk values is due to the possible tensile strain effect that the substrate can induce in the film lattice structure [39]. This effect is more pronounced for very thin films where the crystal lattice is completely strained on the substrate and it reduces for higher thicknesses where the lattice parameters relax towards the bulk values [40]. Because the LCMO layers in the trilayers are thicker than 80 Å, a T_{MI} value higher than 145 K and T_M higher than 125 K are expected at least if only strain effects are taken into account. A similar argument can be applied to the YBCO layers deposited in the trilayers structure where in both the samples the thickness is higher than 100 Å expecting a T_c value higher than 78 K. The $h-l$ X-ray map shown in Figure 3b gives a further confirmation of our hypothesis since LCMO grows strained on the substrate as in the case of thin films and YBCO grows fully relaxed.

Our experimental data show that the proximity between LCMO and YBCO layers reduces T_c, gives rise to an upward curvature in $H_{c2}(T)$ and strongly depresses the activation energy. Although LCMO and YBCO are respectively magnetic and superconducting as previously discussed, all the observed phenomena could also be ascribed to the presence of thermal fluctuations, secondary phases or oxygen vacancies in YBCO. Apart the thermal fluctuations, which are particularly significant in the case of thin films [34], the formation of secondary phases can be neglected on the basis of X-ray diffraction analysis which show a good crystalline quality. Moreover the possible lack of oxygen in YBCO, which can be due to a migration of these atoms towards the LCMO layers during the deposition process, can also be excluded. In fact,

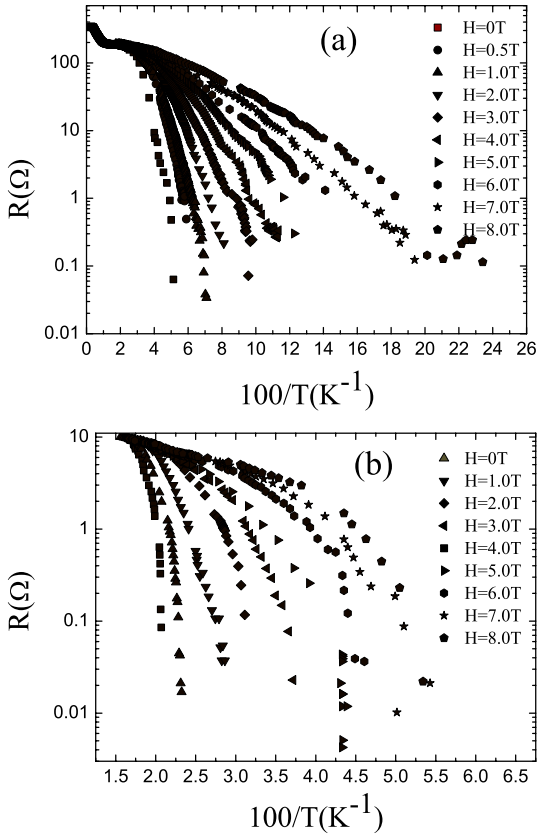

Fig. 6. Arrhenius plot of the data shown in Figure 4a (a) and in Figure 4b (b) respectively.

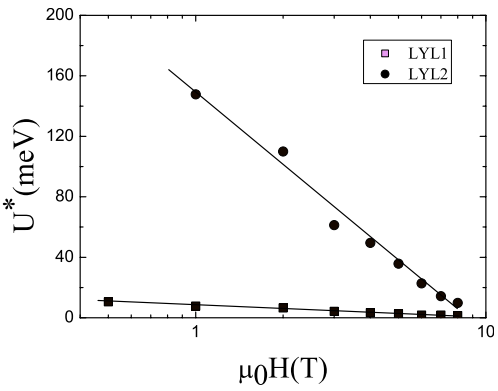

Fig. 7. Activation energy vs. external magnetic field as obtained from the slope of the Arrhenius plot shown in Figure 6 for the two samples.

the measurement of the c-axis length for $YBa_2Cu_3O_{7-\delta}$ in the LYL1 sample gives $\delta \cong 0.22$ which corresponds to $T_c \cong 84$ K as obtained from the universal relationships between T_c, δ and c for this material [41]. These observations give a strong indication that the observed phenomena can be ascribed to proximity between magnetic LCMO and superconducting YBCO layers.

As previously emphasized referring to the $H-T$ phase diagram, the temperature dependence of the IL indicates that the dissipation region is governed by TAFF. Based on this assumption, the ILs represent the values of the field and temperature when the activation energy U is comparable to k_BT. Below this line, U is proportional to the vortex lattice correlated volume $V_c = L_cR_c^2$ where R_c and L_c are the correlation lengths parallel and perpendicular to the $a-b$ planes of the layers respectively. R_c can be approximated by the distance between the vortices $a_0 = (1.5\phi_0/B)^{1/2}$ which ranges form 170 Å to 550 Å for fields between 1 T and 8 T. The value of L_c allows us to estimate the dimensionality of the vortex lattice which is 2-dimensional (2D) or 3-dimensional (3D) depending if L_c is greather or smaller than the layer thickness. Because the estimated value of L_c in the case of YBCO is about 450 Å [27], for thickness smaller than this value the system behaves 2D and L_c is considered to be equal to the layer thickness. For layers thicker than 450 Å, the system is 3D and $L_c = 450$ Å is assumed. Therefore, the reduction of the superconducting layer thickness involves a transition between the two regimes with a decrease of L_c and consequently of U. Following these arguments, one should expect a 2D behavior for the sample LYL1 where the YBCO layer thickness is 160 Å and a 3D vortex lattice for the sample LYL2 with 660 Å of YBCO. On the contrary, the data in Figure 7 show that the activation energy dependence from the external magnetic field is logarithmic in both cases, indicating the same vortex dynamics independent of the YBCO thickness. As already mentioned, the $U \sim -\log H$ dependence has been widely studied both theoretically and experimentally and, in spite of the different mechanisms that are assumed to give rise to this dependence, all the studies converge towards the conclusion that this dependence indicates a 2D regime of the vortex dynamics.

An interpretation of this 2D behavior can also be given by assuming a reduced carrier density of YBCO resulting on charge transfer at the interfaces when oxide layers are formed during the deposition process [42,43]. However, this does not seem the case of our samples as the reflectivity data shown in Figure 1 suggest. The simulated spectrum is obtained, in fact, using only the LCMO/YBCO/LCMO structure while the introduction of any possible oxide compound at the interfaces gave simulated results not in agreement with the observed data suggesting that the effect of oxide on the dimensionality of vortex lattice, if exist, is negligible in the case of our samples.

A vortex lattice 2D behavior is also observed in the case of deoxygenated $YBa_2Cu_3O_{7-\delta}$ with $7-\delta \leq 6.4$ [42]. Although we do not directly measure the oxygen concentration in YBCO layers, our high angle $\vartheta - 2\vartheta$ X-ray measurements allowed to estimate a value for $\delta = 0.22$ which gives $7-\delta = 6.78$ realizing a negligible charge effect at least if compared with the results of reference [42].

The apparent discrepancy between the U vs. H behavior found in our samples, which is consistent with a 2D vortex lattice, and the expected different regimes due to the YBCO thickness smaller and larger than $L_c \cong 450$ Å in LYL1 and LYL2 samples respectively, can be tentatively understood if one assumes that the proximity between F-LCMO and S-YBCO layers has the effect of reducing the effective YBCO thickness, that is the part of the YBCO layer which maintains its superconducting properties. This hypothesis is consistent with the observation of quasiparticles injection from F into S layer which has been demonstrated by other authors [6,15] investigating the T_c vs. YBCO thickness in LCMO/YBCO/LCMO system. As in our case, the authors compare their results with those observed in PrBCO/YBCO and conclude that the proximity of LCMO with YBCO causes a reduction of the thickness of the superconducting layer which is evidenced in a strong depression of the critical temperature. The effect is mainly attributed to the injection of spin polarized particles from LCMO to YBCO which acts as a pair breaking mechanism extending over a spin diffusion length $l_S = (l_0 v_F \tau_S)^{1/2}$ deep inside the superconductor [6]. Here l_0 is the electron mean free path, v_F is the Fermi velocity and τ_S is the spin polarized quasi particle diffusion time. Taking as typical values $l_0 = 50$ Å, $v_F = 10^7$ cm/s and $\tau_S = 10^{-13}$s, the value of the spin diffusion length results to be 70 Å. Because YBCO is sandwiched between two LCMO layers, a reduction of about 140 Å of the whole YBCO layer is expected for both the samples. This gives an effective thickness of the YBCO layers of about 20 Å and 520 Å for LYL1 and LYL2 samples respectively. Comparing these values with L_c, one can conclude that this qualitative argument gives reason of the 2D behavior observed in the U vs. H dependence for both the samples. A much more marked 2D behavior is obtained if we take into account the results shown in reference [15] where a spin diffusion length of about $3l_S$ is calculated giving a much less effective YBCO superconducting thickness.

However, one important observation has to be made in accepting this model for our data. Because the presence of LCMO layers reduces the superconducting layer thickness to an effective one, one should expect T_c values in zero field comparable to that observed in the case of YBCO/PrBCO multilayers [44] with the YBCO thickness close to the effective thickness in our LCMO/YBCO. This hypothesis comes from the absence of any magnetic induced depairing mechanism in the YBCO/PrBCO system because PrBCO is insulating rather than ferromagnetic. Following reference [44] a T_c value of about 60 K and 90 K should be observed in the case of LYL1 and LYL2 respectively. On the contrary, our resistance vs. temperature measurements show that T_c in zero field are 20 K and 39 K respectively in agreement with YBCO/LCMO bilayers [15]. This suggests that quasi particle spin injection, if it exists, could be not the only mechanism which

plays a role in the LCMO/YBCO system, but another pair breaking mechanism should be invoked.

5 Conculsions

We have studied the dependence of the activation energy on the external magnetic field in LCMO/YBCO/LCMO trilayers with two different YBCO layer thickness. The experimental data, extracted by resistive measurements, have been compared with the data obtained for YBCO/PrBCO multilayers with similar layer thickness and, in contrast with them, suggests that the vortex lattice is in a 2D regime even in the case of a thick YBCO layer. This result has been interpreted on the basis of the recent hypothesis on the existence of injection of spin polarized particles from LCMO into YBCO for these systems. As observed by other authors, the interaction between F and S in YBCO/LCMO systems extends to a distance inside S which is much longer than that expected by the current theories, strongly reducing the effective superconducting layer.

References

1. J.J. Hauser, H.C. Theurer, N.R. Werthamer, Phys. Rev. **142**, 118 (1966)
2. J. Aarts, J.M.E. Geers, E. Bruck, A.A. Golubov, R. Coehoorn, Phys. Rev. B **56**, 2779 (1997)
3. Ya.V. Fominov, N.M. Chtchelkatchev, A.A. Golubov, Phys. Rev. B **55**, 15174 (1997)
4. L.R. Tagirov, Physica C **307**, 145 (1998)
5. Th. Muhge, N.N. Garif'yanov, Yu.V. Goryunov, G.G. Khaliullin, L.R. Tagirov, K. Westerholt, I.A. Garifullin, H. Zabel, Phys. Rev. Lett. **77**, 1857 (1996)
6. Z. Sefrioui, D. Arias, V. Pena, J.E. Villegas, M. Varela, P. Prieto, C. Leon, J.L. Martinez, J. Santamaria, Phys. Rev. B **67**, 214511 (2003)
7. V. Peña, Z. Sefrioui, D. Arias, C. Leon, J. Santamaria, M. Varela, S.J. Pennycook, J.L. Martinez, Phys. Rev. B **69**, 224502 (2003)
8. V. Peña, Z. Sefrioui, D. Arias, C. Leon, J. Santamaria, J.L. Martinez, S.G.E. te Velthuis, A. Hoffmann, Phys. Rev. Lett. **94**, 57002 (2005)
9. J.Y.T. Wei, N.-C. Yeh, R.P. Vasquez, Phys. Rev. Lett. **79**, 5150 (1997)
10. M.-H. Ho, N.D. Mathur, N.K. Todd, M.G. Blamire, Phys. Rev. B **61**, R14905 (2000)
11. T. Holden, H.-U. Habermaier, G. Cristiani, A. Golnik, A. Boris, A. Pimenov, J. Humlicek, O.I. Lebedev, G. Van Tendeloo, B. Keimer, C. Bernhard, Phys. Rev. B **69**, 064505 (2004)
12. L.R. Tagirov, Phys. Rev. Lett. **83**, 2058 (1999)
13. T. Kontos, M. Aprili, J. Lesueur, X. Grison, Phys. Rev. Lett. **86**, 304 (2001)
14. V.A. Vasko, V.A. Larkin, P.A. Kraus, K.R. Nikolaev, D.E. Grupp, C.A. Nordman, A.M. Goldman, Phys. Rev. Lett. **78**, 1134 (1997)
15. S. Soltan, J. Albrecht, H.U. Habermeier Phys. Rev. B **70**, 144517 (2004)
16. A.N. Lykov, Adv. Phys. **42**, 263 (1993)
17. C. Coccorese, C. Attanasio, L.V. Mercaldo, M. Salvato, L. Maritato, J.M. Slaughter, C.M. Falco, S.L. Prischepa, B.I. Ivlev, Phys. Rev. B **57**, 7922 (1998)
18. G. Blatter, M.V. Feigel'man, L.B. Geshkenbein, A.I. Larkin, Rev. Mod. Phys. **66**, 1125 (1994)
19. J.R. Clem, Phys. Rev. B **43**, 7837 (1991)
20. T.T.M. Palstra, B. Batlogg, R.B. van Dover, L.F. Schneemeyer, J.V. Waszczak Phys. Rev. B **41**, 6621 (1990)
21. C.J. Van der Beek, P.H. Kes, Phys. Rev. B **43**, 13032 (1991)
22. C. Attanasio, C. Coccorese, V.N. Kushnir, L. Maritato, S.L. Prischepa, M. Salvato, Physica C **255**, 239 (1995)
23. M. Inui, P.B. Littlewood, S.N. Coppersmith, Phys. Rev. Lett. **63**, 2421 (1989)
24. T. Matsushita, T. Fujiyoshi, K. Toko, K. Yamafuji, Appl. Phys. Lett. **56**, 2039 (1990)
25. M.V. Feigel'man, V.B. Geshkenbein, A. Larkin, Physica C **167**, 177 (1990)
26. H. Obara, A. Sawa, S. Kosaka, Phys. Rev. B **49**, 1224 (1994)
27. O. Brunner, L. Antognazza, J.M. Triscone, L. Miéville, Ø. Fisher, Phys. Rev. Lett. **67**, 1354 (1991)
28. Y. Suzuki, J.M. Triscone, M.R. Beasley, T.H. Geballe, Phys. Rev. B **52**, 6858 (1995)
29. D. Ravelosona, J.P. Contour, N. Bontemps, Phys. Rev. B **61**, 7044 (2000)
30. L.G. Parrat, Phys. Rev. **95**, 359 (1954)
31. L. Nevot , P. Croce, Rev. Phys. Appl. **15**, 761 (1980)
32. M. Salvato, A. Vecchione, A. De Santis, F. Bobba, A.M. Cucolo, J. Appl. Phys. **97**, 103712 (2005)
33. Z.Q. Yang, R. Hendrikx, J. Aarts, Y. Qin, H.W. Zandbergen, Phys. Rev. B **67**, 024408 (2003)
34. L.N. Bulaevskii, V.L. Ginzburg, A.A. Sobyanin, Sov. Phys. JETP **67**, 1499 (1988)
35. L.F. Cohen, H.J. Jensen, Rep. Prog. Phys. **60**, 1581 (1997)
36. M. Thinkam, Phys. Rev. Lett. **61**, 1658 (1988)
37. Y. Yeshurun, A.P. Malozemoff, Phys. Rev. Lett. **69**, 2202 (1988)
38. E. Zeldov, N.M. Amer, G. Koren, A. Gupta, R.J. Gambino, M.W. McElfresh, Phys. Rev. Lett. **62**, 3093 (1989)
39. W. Prellier, Ph. Lecoeur, B. Mercey, J. Phys.: Condens. Matter **13**, R915 (2001)
40. R.B. Praus, B. Leibold, G.M. Gross, H.-U. Habermeier, Appl. Surf. Science **138**, 40 (1999)
41. J.D. Jorgensen, B.W. Veal, A.P. Paulikas, L.J. Nowicki, G.W. Crabtree, H. Claus, W.K. Kwock, Phys. Rev. B **41**, 1863 (1990)
42. Z. Sefrioui, D. Arias, M. Varela, J.E. Villegas, M.A. Lopez de la Torre, C. Leon, G.D. Loos, J. Santamaria, Phys. Rev. B **60**, 15423 (1999)
43. Y. Muraoka, T. Muramatsu, J. Yamaura, Z. Hiroi, Appl. Phys. Lett. **85**, 2950 (2004)
44. T. Terashima, K. Shimura, Y. Bando, Phys. Rev. Lett. **67**, 1362 (1991)